


**CASE IMAGE**

# A 57-year-old woman with falls, slurred speech, and abnormal MRI signal in the pons, middle cerebellar peduncles, and cerebellum

Ashley Holloman<sup>1</sup> | Shyam Panchal<sup>2</sup> | Eva Mistry<sup>3</sup> | Paloma Monroig-Bosque<sup>1</sup> | Paul Christensen<sup>1</sup> | Eugene Lai<sup>2</sup> | Matthew Cykowski<sup>1,2</sup> 

<sup>1</sup>Department of Pathology and Genomic Medicine, Houston Methodist Hospital, Houston, Texas, USA

<sup>2</sup>Stanley H. Appel Department of Neurology, Houston Methodist Hospital, Houston, Texas, USA

<sup>3</sup>Department of Neurology and Rehabilitation Medicine, University of Cincinnati, Cincinnati, Ohio, USA

**Correspondence**

Matthew Cykowski, Houston Methodist Hospital, 6565 Fannin Street, Room 227, Houston, TX 77030, USA.

Email: [mdcykowski@houstonmethodist.org](mailto:mdcykowski@houstonmethodist.org)

## 1 | CLINICAL HISTORY

A 57-year-old woman with a one-year history of frequent falls was evaluated for progressive gait instability. Past medical history was significant for hypertension and pulmonary embolism, and the patient was previously evaluated for “stroke” at an outside institution. CT brain identified cerebellar edema. MRI brain revealed abnormal hyperintensities in the bilateral cerebellar hemispheres, pons, and middle cerebellar peduncles on T2-weighted imaging (Figure 1A), with heterogeneous

**BOX 1 Slide scan**

Access the whole slide scan at <http://image.upmc.edu:8080/NeuroPathology/BPA/BPA-21-08-213/view.apml?>

post-contrast enhancement on T1-weighted imaging (Figure 1B). CT of the chest, abdomen, and pelvis revealed thickening of the left renal pelvis, concerning for

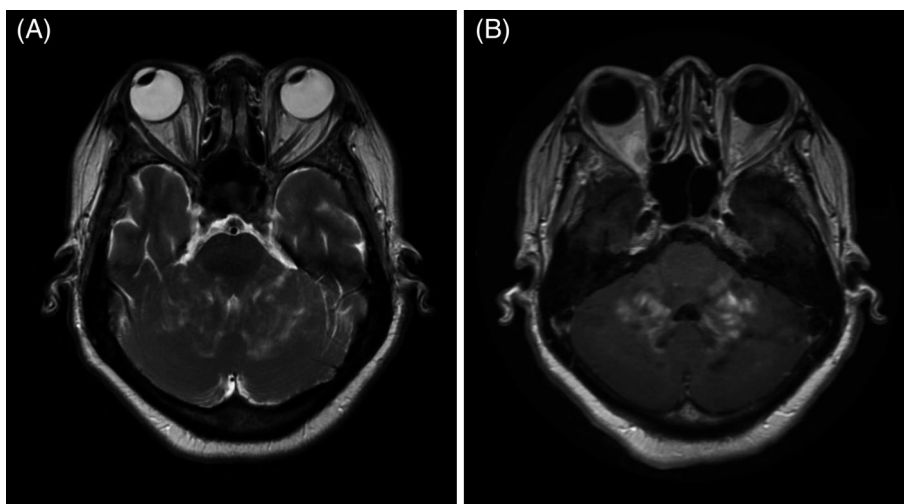


**FIGURE 1** MRI brain, axial sections. (A) T2-weighted MRI demonstrated abnormal hyperintensities in the bilateral cerebellar hemispheres, pons, and the middle cerebellar peduncles. (B) T1-weighted imaging with contrast showed patchy enhancement. No diffusion restriction was present (not shown). The radiologic differential diagnosis included hematopoietic neoplasms, metastatic disease, and atypical demyelinating disease

This is an open access article under the terms of the [Creative Commons Attribution-NonCommercial-NoDerivs](https://creativecommons.org/licenses/by-nc-nd/4.0/) License, which permits use and distribution in any medium, provided the original work is properly cited, the use is non-commercial and no modifications or adaptations are made.

© 2022 The Authors. *Brain Pathology* published by John Wiley & Sons Ltd on behalf of International Society of Neuropathology.

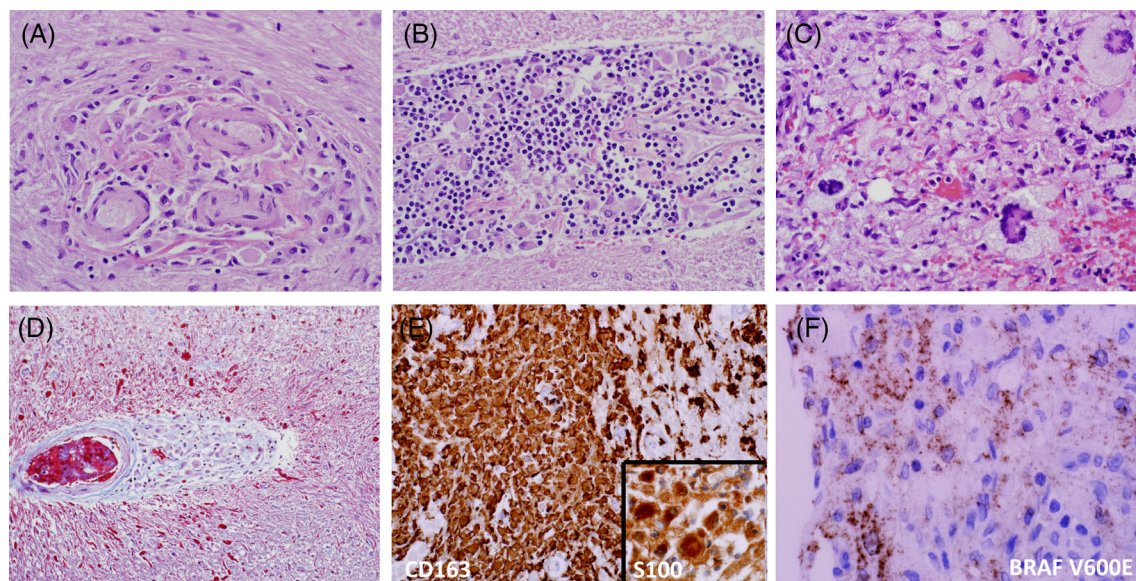


**FIGURE 2** Autopsy findings. H&E-stained sections showed histiocyte-rich lesions in perivascular spaces of pons (A) and within the pontine tegmentum (B), with admixed lymphocytes. Outside of the brain, histiocyte-rich lesions were seen in the renal pelvis (C), with multinucleated Touton giant cells, and within calvarium (not shown). Numerous Rosenthal fibers were seen in deep cerebellar white matter, highlighted by Masson trichrome stain (D). Within cerebellar parenchyma and in perivascular spaces, there were numerous CD163-positive histiocytes (E), and these had weak-to-moderate S100 immunoreactivity (E, inset). The histiocytes were positive for BRAF V600E mutant protein by immunohistochemistry (F) and sequencing. Note the patchy, granular staining in Erdheim-Chester disease with a *BRAF* V600E mutation

carcinoma, and fullness of the right renal pelvis. Scattered mixed sclerotic and lytic lesions in axial skeleton were identified, concerning for metastases. Neurosurgery consult resulted in a biopsy of the cerebellar lesions, with clinical and radiologic concern for metastatic disease. The biopsies revealed only reactive gliosis, Rosenthal fibers, and no neoplastic process. Several months following this evaluation, the patient presented in cardiac arrest and expired. A complete autopsy was requested.

## 2 | FINDINGS

At autopsy, examination of the kidneys was remarkable for firm, tan-yellow, plaque-like lesions in the renal pelvis that involved the renal papillae and extended into the fat of the renal sinuses. No similar cardiac, liver, lung, splenic, or other parenchymal lesions were identified grossly. Examination of the skull revealed a destructive and hemorrhagic lesion in the vertex, as well as the suboccipital craniotomy site from the recent biopsy. Convexity dura was remarkable for multiple discrete, firm, tan-yellow plaque-like lesions on the left convexity dura, resembling those seen in the renal pelvis. Sections through the brainstem and cerebellum revealed firm, ill-defined, and yellow-tan lesions involving the bilateral middle cerebellar peduncles and cerebellum, obscuring the deep cerebellar nuclei. No lesions were seen in the sella, spinal cord, or in coronal sections through cerebrum, ventricles, and subcortical nuclei.

H&E-stained sections of the firm pontine lesion showed histiocyte-rich lesions in perivascular spaces of basis pontis (Figure 2A) and pontine tegmentum

(Figure 2B and Box 1). Histiocyte-rich lesions with multinucleated Touton giant cells were also seen outside the CNS, including within renal pelvis (Figure 2C and Box 1). The middle cerebellar peduncles, cerebellar white matter, and deep cerebellar nuclei were also involved by a perivascular and parenchymal histiocytic infiltrate with associated reactive gliosis. There was prominent Rosenthal fiber formation in the cerebellar white matter, highlighted by Masson trichrome stain (Figure 2D). Foamy perivascular and parenchymal histiocytes were highlighted by CD163 immunostain (Figure 2E), Factor XIIIa (not shown), and focally, by S100 (Figure 2E, inset). CD1a was negative. Histiocyte-rich lesions with Touton giant cells were also seen in the skull lesion, as well as within the dural plaques. **What is the diagnosis?**

## 3 | FINAL DIAGNOSIS

Erdheim-Chester disease (ECD), with *BRAF* V600E mutation demonstrated by both sequencing and immunohistochemistry (Figure 1F).

## 4 | DISCUSSION

Erdheim-Chester disease (ECD) is a rare histiocytosis that most commonly affects middle-aged adults. ECD has conventionally been considered a type of “non-Langerhans cell histiocytosis,” along with Rosai–Dorfman disease and juvenile xanthogranuloma. A recently revised classification of histiocytoses placed ECD in the “L” (Langerhans)

group, and specifically within the indeterminate cell histiocytosis (ICH) subtype of the “L” group [1]. This classification scheme recognizes the common molecular underpinnings of both Langerhans cell histiocytosis (LCH) and ECD, with *MAPK* pathway mutations common to both, as well as those occasional cases with features of both entities (“mixed LCH/ECD”). In the present case, no features of LCH were present and CD1a was negative. As such, the present case represents a classic form of ECD, with involvement of CNS, dura, renal pelves and skeleton (see above). Spleen, small bowel, lung, and esophagus were also involved by ECD on microscopic examination.

The clinical presentation of ECD is variable, although skeletal involvement with sclerotic lesions in the lower extremity is nearly universal [1,2]. CNS involvement occurs in 25–50% of patients [2], and the most frequently involved structures are the pons, middle cerebellar peduncles (MCPs), and deep cerebellar nuclei and cerebellar white matter. This distribution may result in ataxia and stroke-like symptoms, as seen in this patient. In addition, CNS involvement commonly includes dura (present in this case), as well as the hypothalamus-pituitary axis, with associated diabetes insipidus (absent in this case).

Corresponding to this distribution of lesions, MRI studies may demonstrate both intra-axial and extra-axial lesions. Particularly in the posterior fossa, ECD-lesions appear hyperintense on T2-weighted imaging (pons, MCPs, and cerebellum) and demonstrate irregular contrast enhancement (Figure 1). This may include transversely oriented enhancement in the pons [3], although that pattern was not seen here. The radiologic differential diagnosis of ECD may therefore include metastatic disease, lymphoma, inflammatory or demyelinating diseases, as well as gliomas [3] (all suggested in this patient prior to the final diagnosis).

Histopathologic examination in ECD reveals foamy, lipid-laden histiocytes in a background of fibrosis with scattered Touton giant cells (Figure 2). Rosenthal fiber formation in affected brain regions is common (Figure 2D) and was even present in the non-diagnostic premortem biopsy (not shown). Diffuse CD68, CD163, and Factor XIIIa immunoreactivity are observed. S100 immunoreactivity is also well described in a subset of cases [1], and thus cannot be used in isolation to distinguish between Rosai–Dorfman disease and ECD. CD1a and Langerin are negative, except in examples of mixed LCH/ECD. In the setting of a *BRAF* V600E mutation, first demonstrated by sequencing in this case, immunostain for mutant *BRAF* V600E protein will reveal immunoreactivity. As shown in Figure 1F, the granular cytoplasmic staining for mutant *BRAF* V600E protein can be patchy and easily overlooked.

Molecular studies have identified recurrent alterations in the MAPK and PI3K pathways in patients with ECD [1,2]. Among these, *BRAF* V600E mutations are the most

common alteration identified. Mutations in *MAP2K1*, *NRAS*, *KRAS*, and *PIK3CA* are also described [1,2]. The presence of a *BRAF* alteration allows for the potential use of targeted BRAF-inhibitor therapy, such as vemurafenib. Additional therapies considered may include inhibitors of the MAPK–ERK pathway (MEK inhibitors) and immunosuppressive agents (interferon- $\alpha$ -2a) [2].

## KEYWORDS

*BRAF* V600E, histiocytosis, middle cerebellar peduncles, rosenthal fibers, touton giant cells

## CONFLICT OF INTEREST

None.

## AUTHOR CONTRIBUTIONS

AH, SP, and MC wrote the manuscript. PM-B, PC, and MC performed the autopsy and contributed pathologic expertise to the work, and SP, EM, and EL assessed the patient, and contributed neurologic expertise to the work. MC takes primary responsibility for the accuracy of the information presented. All authors approved the final version of the manuscript.

## DATA AVAILABILITY STATEMENT

Data sharing is not applicable. A scanned whole slide of the characteristic lesions from the autopsy is available (see Box 1).

## ORCID

Matthew Cykowski  <https://orcid.org/0000-0002-5973-803X>

## REFERENCES

- Emile JF, Abba O, Fraitag S, Horne A, Haroche J, Donadieu J, et al. Revised classification of histiocytoses and neoplasms of the macrophage-dendritic cell lineages. *Blood*. 2016;127(22):2672–81. <https://doi.org/10.1182/blood-2016-01-690636>
- Goyal G, Heaney ML, Collin M, Cohen-Aubart F, Vaglio A, Durham BH, et al. Erdheim-Chester disease: consensus recommendations for evaluation, diagnosis, and treatment in the molecular era. *Blood*. 2020;135(22):1929–45. <https://doi.org/10.1182/blood.2019003507>
- Sedrak P, Ketonen L, Hou P, Guha-Thakurta N, Williams MD, Kurzrock R, et al. Erdheim-Chester disease of the central nervous system: new manifestations of a rare disease. *Am J Neuroradiol*. 2011;32:2126–31.

**How to cite this article:** Holloman A, Panchal S, Mistry E, Monroig-Bosque P, Christensen P, Lai E, et al. A 57-year-old woman with falls, slurred speech, and abnormal MRI signal in the pons, middle cerebellar peduncles, and cerebellum. *Brain Pathology*. 2022;32:e13072. <https://doi.org/10.1111/bpa.13072>